of PVF_2 homopolymer does not undergo a similar solid-state transformation during electron irradiation, but degrades directly to an amorphous structure. This discrepancy in behavior between homopolymer and copolymers is correlated with molecular and crystallographic differences that allow greater freedom of intramolecular bond rotations in the latter. Single crystals of these copolymers grown at high temperatures lack distinct growth facets, as was also found earlier for poly(trifluoroethylene); this morphological irregularity is ascribed in both cases to chemical, configurational, and conformational disorder. Dark-field electron microscopy at room temperature shows the copolymer lamellae to consist of small, fragmented crystallites, which, however, combine into larger, coherently scattering areas during electron irradiation. This fragmentation is attributed to lattice changes accompanying the paraelectric-to-ferroelectric transformation during cooling of the crystals to room temperature, while the subsequent electron-induced healing is ascribed to the return to a structural analogue of the original paraelectric lattice.

Registry No. (VF_2)-(F_3E) (copolymer), 28960-88-5; (VF_2)-(F_4E) (copolymer), 25684-76-8.

References and Notes

(1) Furukawa, T.; Johnson, G. E.; Bair, H. E.; Tajitsu, Y.; Chiba, A.; Fukada, E. *Ferroelectrics* **1981**, *32*, 61.
(2) Higashihata, Y.; Sako, J.; Yagi, T. *Ferroelectrics* **1981**, *32*, 85.
(3) Lovinger, A. J.; Furukawa, T.; Davis, G. T.; Broadhurst, M. G. *Polymer* **1983**, *24*, 1225, 1233.
(4) Tashiro, K.; Takano, K.; Kobayashi, M.; Chatani, Y.; Tadokoro, H. *Polymer* **1983**, *24*, 199.
(5) Lovinger, A. J. *Macromolecules* **1983**, *16*, 1529.
(6) Lovinger, A. J.; Johnson, G. E.; Bair, H. E.; Anderson, E. W. *J. Appl. Phys.* **1984**, *56*, 2412.
(7) Lando, J. B.; Doll, W. W. *J. Macromol. Sci., Phys.* **1968**, *B2*, 205.
(8) For a general review, see: Lovinger, A. J. *Science* **1983**, *220*, 1115 and references therein.
(9) Grubb, D. T. *J. Mater. Sci.* **1974**, *9*, 1715.
(10) Orth, H.; Fischer, E. W. *Makromol. Chem.* **1965**, *88*, 188.
(11) Kobayashi, K.; Sakaoku, K. *Lab. Invest.* **1965**, *14*, 1097.
(12) Kiho, H.; Ingram, P. *Makromol. Chem.* **1968**, *118*, 45.
(13) Thomas, E. L.; Sass, S. L. *Makromol. Chem.* **1973**, *164*, 333.
(14) Keller, A. *J. Polym. Sci.* **1959**, *36*, 361.
(15) Chacko, V. P.; Adams, W. W.; Thomas, E. L. *J. Mater. Sci.* **1983**, *18*, 1999.
(16) Sakaoku, K.; Peterlin, A. *J. Macromol. Sci., Phys.* **1967**, *B1*, 401.
(17) Willems, *J. Discuss. Faraday Soc.* **1958**, *25*, 111.
(18) Yagi, T.; Tatemoto, T. *Polym. J.* **1979**, *11*, 429.
(19) Lovinger, A. J.; Cais, R. E. *Macromolecules* **1984**, *17*, 1939.

Electron Paramagnetic Resonance Investigation of Orientation Produced by Mechanical Processing in the Fillers of Polymer Composites

Antal Rockenbauer,* László Jókay, Béla Pukánszky, and Ferenc Tüdös

Central Research Institute for Chemistry, Hungarian Academy of Sciences, H-1525 Budapest, Hungary.

Received June 18, 1984

ABSTRACT: Electron paramagnetic resonance spectroscopy has been applied in order to study the orientation effects of mechanical deformation of the calcium carbonate fillers of polymer composites. The anisotropic signals of Mn^{2+} ions substituting Ca^{2+} ions and electron defect centers in calcium carbonate served as spin probes in these studies. The morphology of the calcium carbonate crystallites was found to play a dominant role in the effectivity of ordering. Because of the mechanical deformations, the *c* crystallographic axis of calcite is preferentially perpendicular to the plane of compression molding and the direction of stretching in a variety of polymer composites of low-density polyethylene, polypropylene, impact-resistant polystyrene, and plasticized poly(vinyl chloride) containing different additives.

Introduction

The electron paramagnetic resonance (EPR) method has been recently applied to the study of the orientation in the amorphous regions of polymers.[1-3] In this work paramagnetic molecules were introduced into the amorphous region of elongated polymer films and the order parameter of the partially oriented molecules was derived from the angular dependence of the EPR spectra.

We have also developed an EPR method in order to investigate the mechanically produced orientation of the fillers in polyethylene composites.[4] In this case the Mn^{2+} impurity centers and the trapped electrons in the filler served as natural "spin probes". The advantage of our method is that beside the experimental simplicity (no irradiation and sophisticated chemical treatment is required for introducing the probing additives and the samples can be investigated at room temperature) the investigated orientation effects characterize directly the interactions between the crystallites of the filler and the polymer chain, which plays a dominant role in the modifications of mechanic properties of the polymer composites.

In this paper the orientational properties of some industrial fillers (Durcal 2 and Millicarb; milled $CaCO_3$)[5] were studied and methods are developed for the complex characterization of the orientation produced by the compression molding and stretching of different polymer composites. The degree of orientation is compared for polyethylene (PE), polypropylene (PP), polystyrene (PS), and plasticized poly(vinyl chloride) (PVC) composites. The effect of an elastomer (EPDM) is also studied.

Experimental Section

Polymer Composites. The following compounds were used: PE, 80 wt % low-density polyethylene (Typolen: FA 2210, TVK, Hungary) and 20 wt % filler (Durcal 2, milled $CaCO_3$ with average particle diameter 3 μm, produced by Omya); PP/1, 80 wt % polypropylene (ethylene–propylene copolymer with an ethylene content less than 5%, TVK, Hungary; Typolen K 501) and 20 wt % filler (Durcal 2); PP/2, 70 wt % polypropylene (K 501),

0024-9297/85/2218-0918$01.50/0

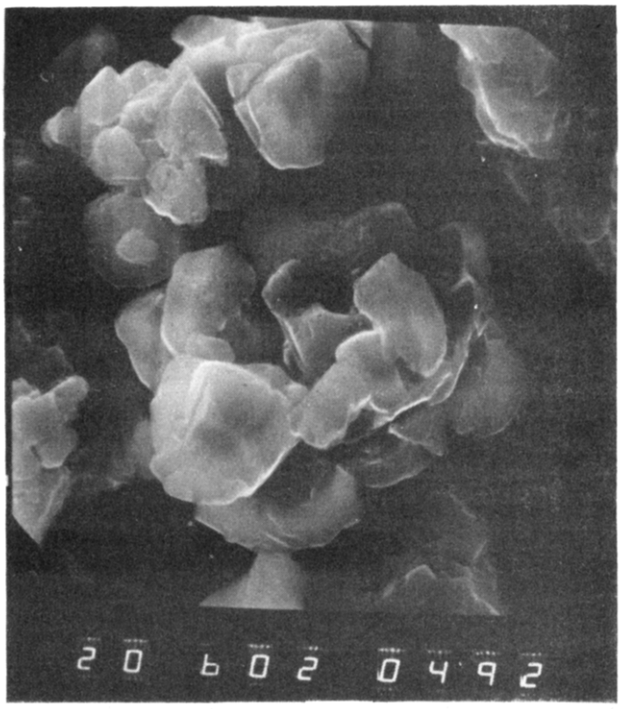

Figure 1. Electron-microscopic picture of Dural 2 powder. Magnification: 6000 times.

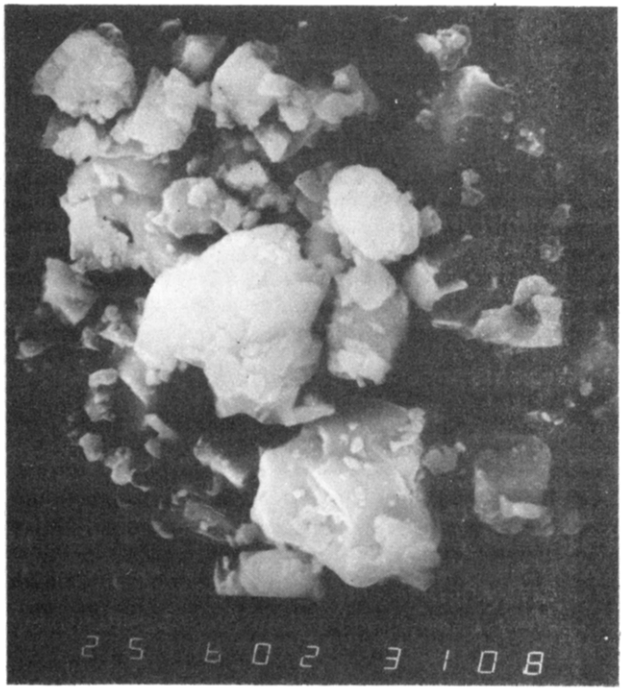

Figure 2. Electron-microscopic picture of Millicarb powder. Magnification: 6000 times.

20 wt % Durcal 2, and 10 wt % elastomer (Buna AP 447, Hüls, FRG); PP/3, 75 wt % polypropylene (K 501), 15 wt % Millicarb (milled $CaCO_3$ with average particle diameter 3 μm, Omya), and 10 wt % elastomer (Vestapren 2047, Hüls, FRG); PVC, 60 wt % suspension poly(vinyl chloride) (Ongrovil S 5167, BVK, Hungary), 20 wt % filler (Durcal 2), and 20 wt % plasticizer (Eviplast 80: diisooctyl phthalate, EVM, Hungary); PS, 80 wt % impact-resistant polystyrene (Krasten 336, Czechoslovakia) and 20 wt % Durcal 2.

The above composites also contain stabilizers, required for the processing. The morphology of Durcal 2 and Millicarb is shown on Figures 1 and 2. The electron-microscopic pictures are made by Jeol type JSM-35 scanning equipment with an amplification of 6000.

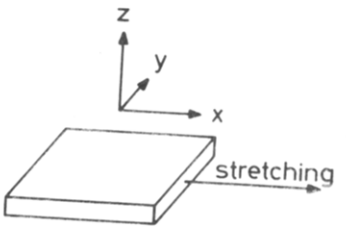

Figure 3. Orientation of the x, y, and z axes with respect to the stretched polymer plate.

Methods. The ingredients of the composites were mixed in a Rheomix 600 mixing chamber of a Haake Rheocord EU 10V plastograph at 50 min^{-1} speed for 10 min. The mixing temperature was 140 °C for the PE, 170 °C for the PS, and 185 °C for the PVC and PP composites. The blends were compression molded to 1 mm thick plates with 25-MPa pressure for 1 min. The temperature of the compression molding was 140 °C for PE, 170 °C for PVC, and 190 °C for PS and PP. From the plates tensile specimens were cut and stretched at 100 mm/min deformation rate. Rectangular plates were cut from the compressed and stretched samples. The plates were stacked and mounted on a goniometer, in which the rotation axis was perpendicular to the direction of magnetic field. The plates were mounted at three different positions: for experiment A, the rotation axis was parallel to the stretching direction (axis x); for experiment B, the rotation axis was perpendicular to the stretching direction and parallel to the plane of compression (axis y); for experiment C, the rotation axis was parallel to the normal of the plate (axis z). The orientation of the x, y, and z axes fixed to the compressed and stretched plate is shown in Figure 3. The EPR spectra were recorded by a Jeol type JES-FE-3X spectrometer in X band with 100-kHz field modulation at room temperature.

EPR Spectra of Fillers. The EPR spectra of both fillers (Durcal 2 and Millicarb) reveal the presence of some transition-metal impurities and defect centers. A characteristic anisotropic signal of Fe^{3+} can be seen at $g = 4.3$ and the nearly equidistant six-line pattern of Mn^{2+} ions at $g = 2.00$ can also be recognized. The defect centers yield a complex pattern in the region $g = 2.00$–2.01. In order to study the orientation of crystallites in the composites any of the paramagnetic centers can be applied as a spin probe if the respective signal reveals substantial anisotropy. The major requirement is that the signal bands, corresponding to the principal directions, should be well separated. Then the amplitude of the respective signal feature is proportional to the number of molecules (or crystallites) in which the respective principal direction (e.g., magnetic symmetry axis) is aligned with the magnetic field. Such resolved bands can be recognized both in the spectrum of Mn^{2+} ion and in the defect centers.

On the basis of magnetic parameters obtained from the spectra of Durcal 2 and Millicarb the Mn^{2+} centers can be assigned to Mn^{2+} ions substituting the Ca^{2+} ions in the calcite crystal lattice. The single-crystal studies of calcite[6] reveal an axial magnetic symmetry with a very small g and hyperfine anisotropy; thus, the spectral anisotropy of a randomly or partially ordered powder of calcite crystallites can be well described by the D axial zero-field parameter.[7] At this approximation the resonance field of the six major allowed transitions ($\Delta M_S = {}^1/_2$ to $-{}^1/_2$ and $\Delta M_I = 0$) can be written as

$$H_{M_I}(\vartheta) = H_0 - AM_I - (A^2/2H_0)(I(I+1) - M_I^2) - 2(D^2/H_0)[(1 - AM_I/H_0)\sin^4\vartheta - 2(1 - 9AM_I/H_0)\sin^2 2\vartheta] \quad (1)$$

where ϑ is the angle between the magnetic field and the c crystallographic axis of calcite, $H_0 = h\nu/g\beta = 333$ mT in our experiments, and $I = {}^5/_2$ for the ^{55}Mn nucleus. The A hyperfine and D zero-field parameters are expressed in magnetic field units: $A = 9.4$ mT and $D = 8.0$ mT.

The angular dependence of the six $M_I = {}^5/_2, {}^3/_2, \ldots, -{}^5/_2$ transitions is described by the last term in eq 1. The resonance can be detected at the smallest field if $\vartheta = 90°$ (perpendicular band) and at the largest field if $\vartheta = 45°$ (nonprincipal band), while the $\vartheta = 0°$ parallel band can be detected at intermediate position. It can also be seen from eq 1 that the separation of zero-field bands depends on the value of M_I: for negative M_I, i.e., for the hyperfine

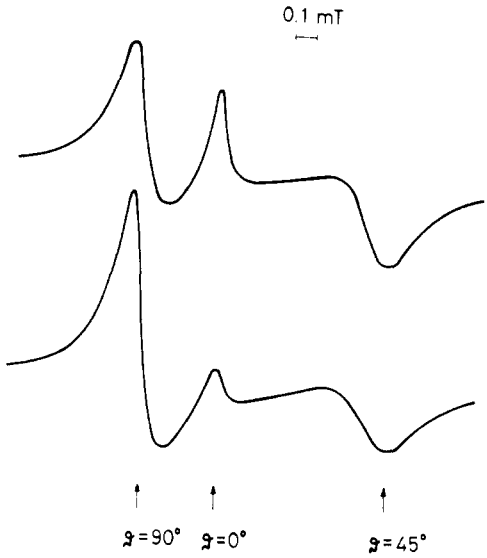

Figure 4. Fourth hyperfine line of Mn^{2+} in the compression-molded PE composite: the magnetic field is perpendicular (top) and parallel (bottom) to the plane of compression.

lines observed in the high-field part of the spectrum, the perpendicular, parallel, and nonprincipal bands are better separated than in the low-field part of the spectrum. For the purpose of orientation measurements we selected the fourth ($M_I = -1/2$) hyperfine line, where the central band (i.e., the parallel band) is not too small and separated by 0.4 mT from the perpendicular and 0.8 mT from the nonprincipal band, respectively (Figure 4).

It is interesting to note that also the Mn^{2+} ions in calcite were applied by Blanchard and Chasteen[8] when they studied the ordering in the prismatic region of a seashell. In their case, however, where the degree of ordering was large the angular dependence manifested itself through the variation of line positions. In our case—similarly to the oriented amorphous polymers studied by Schuch[1,2] as well as Shimada and Williams[3]—the low degree of orientation results in variation of the amplitudes of spectral bands, only.

Both the Durcal 2 and Millicarb possess a complex spectrum of defect centers. As the orientation dependence of these lines is studied only for the Durcal 2, we omit here the analysis of the lines that can be detected only in Millicarb. In the spectra of Durcal 2 four lines can be seen at $g_1 = 2.0053$, $g_2 = 2.0034$, $g_3 = 2.0021$, and $g_4 = 2.0002$, respectively (Figure 5). The line width is rather narrow (ca. 0.02 mT) and no hyperfine splitting can be seen. As a probe signal we selected the lines with $g_2 = 2.0034$ and $g_3 = 2.0021$, where the former has the characteristic shape of a perpendicular band and the latter has that of a parallel band if the powder pattern is determined by an axially symmetric **g** tensor. These bands show angular dependence analogous to the perpendicular and parallel features of the Mn^{2+} centers: the line amplitude at g_2 has a maximum and a minimum at the same orientation as the perpendicular feature of Mn^{2+}. The same holds for the line at g_3 and the parallel feature of the Mn^{2+} spectrum. This observation suggests that the symmetry axis of the defect center yielding the lines at g_2 and g_3 aligns also with the c crystallographic axis of calcite.

Though the origin of defect centers in Durcal 2 is probably connected with the presence of impurities, we can tentatively assign them to the irradiation-produced defect centers in calcite single crystals of low impurity level. The spectra observed in calcite crystals[9-11] were assigned to different molecular ions as CO_2^-, CO_3^-, and CO_3^{3-}, but among them only CO_2^- is stable at room temperature. As concerning the position of bands, however, only the g values of CO_3^{3-} ($g_\perp = 2.0031$ and $g_\parallel = 2.0013$) are in close agreement with g_2 and g_3; therefore, we assume that the center under study in Durcal 2 is a CO_3^{3-} molecular ion stabilized by some impurities (e.g., Fe^{3+}). For this radical the symmetry axis was found to be normal to the plane of CO_3, i.e., parallel to the c crystallographic axis.[10] It is in accordance with our finding that the parallel and perpendicular bands of the Mn^{2+} ions and the defect centers manifest analogous angular variation.

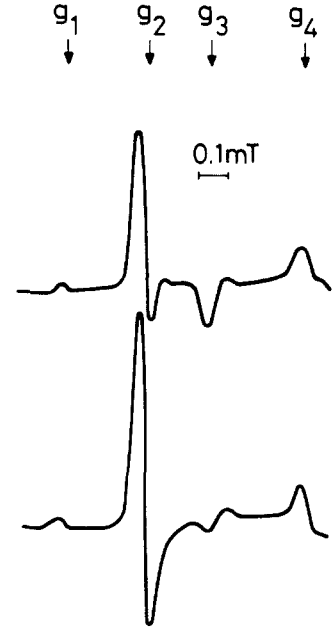

Figure 5. Signal of defect centers in the compression-molded PE composite: the magnetic field is perpendicular (top) and parallel (bottom) to the plane of compression.

Results and Discussion

As has been pointed out in the previous analysis, the amplitudes of the perpendicular and parallel features of Mn^{2+} ions and defect centers are measures of the number of crystallites in which the c axis, i.e., the magnetic symmetry axis, is perpendicular or parallel to the magnetic field. In all of the investigated polymer composites containing Durcal 2 these spectral features show similar angular dependence for the Mn and the defect signal. In the compression-molding experiments if the magnetic field is aligned normal to the plane of compression the amplitude of the parallel band has a maximum and that of the perpendicular band a minimum. On the other hand, when the field is oriented parallel with the plane, the perpendicular band has a maximum and the parallel band a minimum amplitude. In the stretching experiment, if the field is kept normal to the plane of compression in the course of sample rotation (experiment C), the parallel band has a maximum when the field is perpendicular to the stretching direction (i.e., H is aligned with the axis y) and a minimum when it is parallel with the stretching (i.e., H is aligned with the axis x). The perpendicular band presents an opposite angular dependence. Consequently the crystallites of Durcal 2 are oriented by the mechanical deformations in such a way that the c axis of the crystallites always tends to be perpendicular to the direction of deformation (i.e., the plane of compression and the direction of stretching, respectively).

If the polymer composite contains Millicarb as a filler, a much weaker orientation due to the compression molding and stretching can be observed. The trends, however, show similar angular dependence for the parallel and perpendicular features of the Mn^{2+}. The smaller degree of orientation of Millicarb crystallites can be related to the morphology of the fillers. In Figures 1 and 2 the electron microscopic picture of Durcal 2 powder shows some plane portions on the surface of crystallites, while the Millicarb crystallites are more amorphous morphologically.

Some conclusions can also be drawn about the orientation of the magnetic symmetry axis c with respect to the planes of the crystallites. If the filler is oriented by the polymer under stress, these planes should be aligned with

Table I
r_k Values for Mn^{2+} Centers in $CaCO_3$

degree of stretching, %	axis of rotation	r_x	r_y	r_z
	PP/1			
0	xy	0.725	0.725	
23	z	0.420	0.719	
92	z	0.179	1.025	
155	z	0.185	1.124	
187	z	0.205	0.943	
187	x		1.014	2.87
187	y	0.250		2.81
	PP/2			
0	xy	0.722	0.722	
21	z	0.461	0.752	
58	z	0.362	0.813	
98	z	0.356	0.870	
138	z	0.234	0.847	
183	z	0.235	1.044	
224	z	0.240	1.00	
224	x		1.01	2.56
224	y	0.238		2.59
	PP/3			
200	y	0.521		0.962
	PE			
0	xy	0.562	0.562	4.24
18	x		0.481	2.89
18	y	0.552		2.81
18	z	0.565	0.578	
123	z	0.118	0.926	
205	y	0.115		3.91
205	z	0.108	1.235	
278	y	0.087		3.91
278	z	0.084	1.114	
336	x		1.018	3.94
336	y	0.083		3.94
336	z	0.093	1.07	
	PVC			
0	xy	0.481	0.481	5.02
47	x		0.613	5.71
47	y	0.268		5.75
47	z	0.281	0.532	
	PS			
0	xy	0.671	0.671	2.15

Table II
r_k Values for the Defect Centers in $CaCO_3$

degree of stretching, %	axis of rotation	r_x	r_y	r_z
	PP/1			
0	xy	0.855	0.855	2.87
23	z	0.619	1.01	
92	z	0.306	1.58	
155	z	0.353	1.70	
187	z	0.389	1.58	3.86
187	x		1.62	3.51
187	y	0.344		
	PP/2			
0	xy	0.943	0.943	3.28
21	z	0.685	1.045	
58	z	0.578	1.24	
98	z	0.649	1.29	
138	z	0.379	1.50	
183	z	0.382	1.88	
224	z	0.323	1.62	
224	x		1.82	4.95
224	y	0.333		4.51
	PE			
0	xy	0.641	0.641	4.51
18	x		0.625	3.60
18	y	0.662		3.29
18	z	0.633	0.714	
123	y	<0.25		4.93
123	z	<0.25	1.01	
205	y	<0.25		4.55
205	z	<0.25	1.52	
278	y	<0.25		4.65
278	z	<0.25	1.42	
336	x		1.17	5.32
336	y	<0.25		5.38
336	z	<0.25	1.43	
	PVC			
0	xy	0.571	0.571	5.95
47	x		0.709	8.20
47	y	0.238		8.62
47	z	0.254	0.613	
	PS			
0	xy	0.917	0.917	2.60

the direction of deformation; i.e., the normal of planes should be perpendicular to the direction of deformation. As we have found above, the c axis of crystallites is preferentially perpendicular to the direction of deformation; therefore, the c axis either is parallel with the normal of the characteristic plane of crystallites or at least should form a small angle with it. The smaller is the angle, the larger is the degree of orientation that can be obtained in the EPR experiments.

In order to compare the degree of ordering in different polymer composites the variations in amplitude of the perpendicular and parallel features should be measured when the orientation of the sample is changed with respect to the direction of magnetic field. A source of error in direct amplitude measurements is the sensitivity variation of the spectrometer during the sample rotation, which is caused by the displacement of the sample in the microwave cavity. This error can be reduced by averaging for different sample positions with identical angle between the direction of magnetic field and deformation. This method was applied in our previous work.[4] In this paper $I_\parallel/I_\perp$, that is, the amplitude ratio of the parallel and perpendicular features, is investigated, which is independent of the sensitivity of the spectrometer. This ratio can directly characterize the degree of ordering if it is compared with $(I_\parallel/I_\perp)_u$ measured from the spectra of unoriented samples (Durcal 2 powder). We obtained $(I_\parallel/I_\perp)_u = 0.200$ and 0.0667 for the signal of Mn^{2+} and defect centers, respectively. The degree of ordering can be given by the parameters

$$r_k = (I_\parallel/I_\perp)_k/(I_\parallel/I_\perp)_u \quad (2)$$

where the $k = x, y, z$ index refers to the direction of the magnetic field in the frame fixed to the sample plate (see Figure 3). If r_k is larger than 1, the number of crystallites in which the c axis is parallel with the field is enhanced compared to the sample of randomly oriented crystallites. If r_k is smaller than 1, the orientation distribution is reversed.

The values of r_k for different orientations of the composites are summarized in Tables I and II for the Mn^{2+} ions and for the defect centers. Analogous conclusions can be drawn from the two tables. The values of r_x, r_y, and r_z are affected differently by the processings, namely

$$r_x < 1 \qquad r_z > 1 \quad (3)$$

i.e., both the compression and the stretching reduce r_x and increase r_z; on the other hand, $r_y < 1$ if the sample is only compression molded, but when the film is stretched, too, the value of r_y is increased and can exceed 1; i.e., the compression decreases and the stretching increases r_y. These observations suggest that the c magnetic symmetry axis is preferentially perpendicular to the xy plane of the

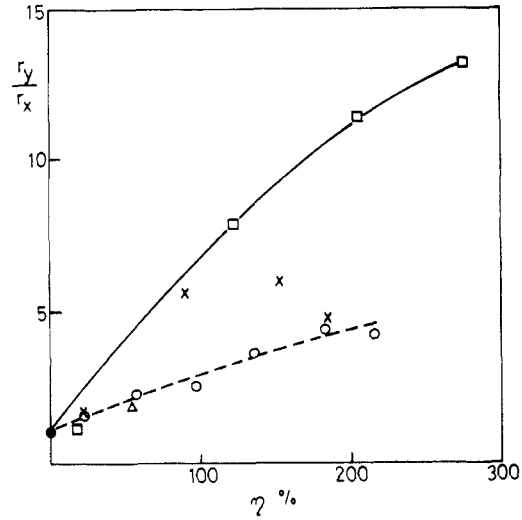

Figure 6. Ratio r_y/r_x for the Mn^{2+} centers vs. the degree of stretching in polymer composites: (□) PE, (×) PP/1, (○) PP/2, (△) PVC.

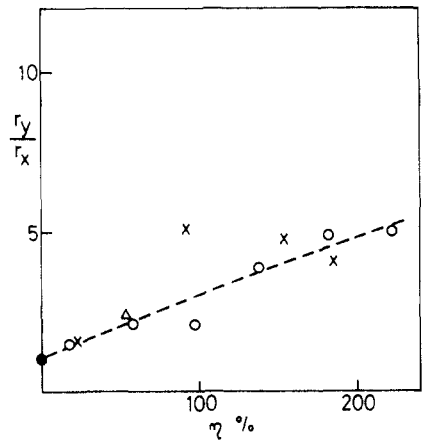

Figure 7. Ratio r_y/r_x for the defect centers vs. the degree of stretching in polymer composites: (×) PP/1, (○) PP/2, (△) PVC.

compression and the x direction of the stretching. Previously we have arrived at the same conclusions when we analyzed the angular dependence of the characteristic features of spectra.

An inverse correlation is expected between the values r_z and r_x: the relative number of crystallites, where the magnetic symmetry axis is parallel with the field, is measured by r_z if the field is normal and by r_x if the field is parallel with the plane of compression molding. The data of Tables I and II are in conformity with this expectation, but for a few entries the large r_z value is not accompanied by small r_x value. It indicates the complex nature of orientation mechanism. By means of EPR spectroscopy the orientation distribution of magnetic symmetry axis is measured with respect to the direction of mechanical processing, but the mechanical processing can produce orientation indirectly by ordering some morphological feature of the crystallites. It means the parameters r_z and r_x depend on two convoluted distributions: (i) the orientation distribution of some morphological feature with respect to the direction of mechanical processing and (ii) the orientation distribution of magnetic axis with respect to the above morphological feature.

The degree of ordering can also be characterized by the ratios r_x, r_y, and r_z; e.g., the ratio r_y/r_x depends only on the orientation produced by the stretching and is independent of the orientation due to the compression molding. That

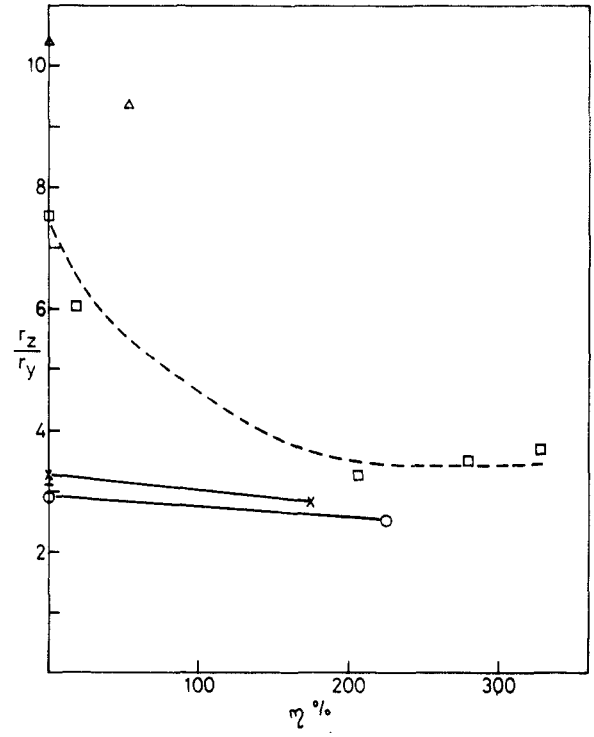

Figure 8. Ratio r_z/r_y for Mn^{2+} centers vs. the degree of stretching in polymer composites: (○) PE, (×) PP/1, (○) PP/2, (△) PVC, (+) PS.

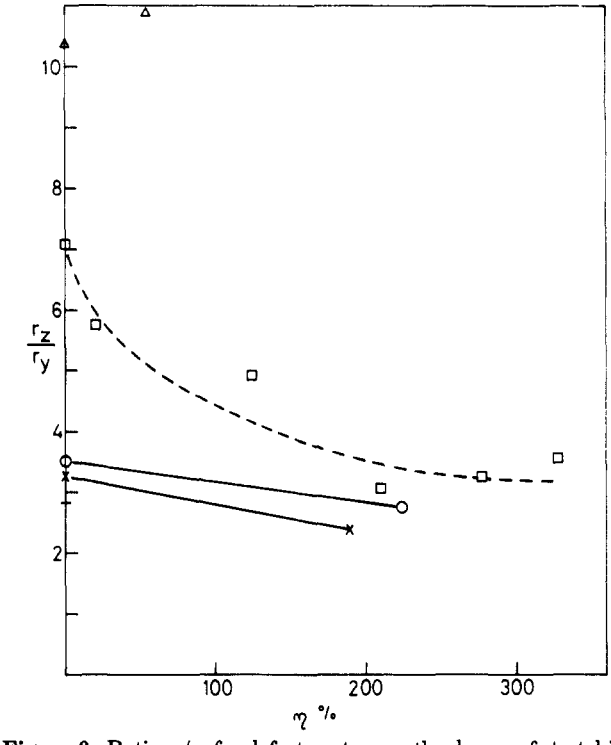

Figure 9. Ratio r_z/r_y for defect centers vs. the degree of stretching in polymer composites: (□) PE, (×) PP/1, (○) PP/2, (△) PVC, (+) PS.

parameter can be obtained via a sample rotation around the z axis, i.e., when the field is set on the plane of compression. On the other hand, the ratio r_z/r_y that can be obtained via a sample rotation around the x direction of stretching being perpendicular to the field characterizes the ordering in the plane of the compression molding.

Figures 6 and 7 show the ratio r_y/r_x calculated from the spectra of the Mn^{2+} ions and the defect centers, respectively, as a function of the stretching degree. In the com-

posite of low-density polyethylene a large and steadily increasing degree of orientation is produced when the degree of stretching is increased. A smaller but still increasing degree of orientation can be observed in the plasticized PVC and elastomer-modified PP. In the composite of PP without elastomer the elongation was not uniform; thus, the degree or ordering cannot be given as a function of the stretching degree.

The r_z/r_y parameters for the Mn^{2+} ion and for the defect centers are plotted against the stretching degree in Figures 8 and 9. If the samples are compression molded without stretching, the degree of orientation varies in the order of PVC > PE > PP ≈ PS. It can be seen—most clearly for the PE composites—that the orientation due to compression molding is partially deteriorated by the subsequent stretching, and a new type of orientation is built up perpendicular to the stretching direction, which yields to the increase of r_y/r_x.

By a few randomly selected examples we have demonstrated that EPR spectroscopy is a useful technique for studying the orientation of fillers for a wide variety of composites. The ordering of polymer composites in the course of mechanical deformations is, however, a rather complex process. It depends on the morphology of the filler and the polymer, the structure of the polymer chain, the temperature and other conditions of the processing and the presence of different additives such as elastomers, plasticizers, etc. Only a systematic study of these factors can elucidate the mechanism of ordering, which can make a valuable contribution to our understanding of the role which the different additives play in the mechanical properties of polymer composites.

Acknowledgment. We are indebted to the R and D department of TVK, Hungary, for the preparation of electron-microscopic pictures of the Durcal 2 and Millicarb powders.

References and Notes

(1) Schuch, H. *Prog. Colloid Polym. Sci.* **1979**, *66*, 87.
(2) Schuch, H. "Preprints of the 26th IUPAC Symposium on Macromolecules, Mainz, 1979"; p 1201.
(3) Shimada, S.; Williams, F. *Macromolecules* **1980**, *13*, 1721.
(4) Rockenbauer, A.; Simon, P.; Pukánszky, B.; Azori, M.; Kelen, T.; Tüdös, F. "29th IUPAC Symposium on Macromolecules, Bucharest, 1983"; Abstracts Vol. IV, pp 211–4.
(5) OMYA Kontakt, Plüss-Staufer AG. Oftringen, Switzerland, 128.
(6) Hurd, F. K.; Sachs, M.; Hershberger, W. D. *Phys. Rev.* **1954**, *93*, 373.
(7) de Wijn, H. W.; van Balderen, R. F. *J. Chem. Phys.* **1967**, *46*, 1381. There is some controversy in the literature about the exact form of higher order perturbation terms. We accepted for formulas of de Wijn and van Balderen, who critically reviewed the perturbation calculations. These authors also pointed out that among the third-order terms only the one which is proportional to AD^2/H_0^2 can give significant contribution.
(8) Blanchard, S. C.; Chasteen, N. D. *J. Phys. Chem.* **1976**, *80*, 1362.
(9) Marshall, S. A.; Reinberg, A. R.; Servay, R. A.; Hodges, J. A. *Mol. Phys.* **1964**, *8*, 225.
(10) Serway, R. A.; Marshall, S. A. *J. Chem. Phys.* **1967**, *46*, 1949.
(11) Serway, R. A.; Marshall, S. A. *J. Chem. Phys.* **1967**, *47*, 868.

Hemitactic Polymers

Mario Farina,* Giuseppe Di Silvestro, Piero Sozzani, and Biagio Savaré

Istituto di Chimica Industriale, Università di Milano, I-20133 Milano, Italy.
Received September 24, 1984

ABSTRACT: Hemitactic polymers constitute a new class of macromolecular stereoisomers in which only one tertiary carbon atom in every two has a definite configuration. The selection rules governing the distribution of stereosequences in such polymers, in particular in hemiisotactic polymers, are discussed together with a probabilistic approach which makes it possible to determine their relative frequencies. The structural features distinguishing hemitactic polymers from conventional atactic polymers and their possible uses are discussed.

After the structure of isotactic and syndiotactic polymers had been brought to light in the mid-1950s, no new form of stereoisomerism in vinyl polymers was observed for a quarter of a century. Since that time, the study of macromolecular stereochemistry has moved ahead in three main directions: synthesis of polymers having complex tacticity (ditactic, tritactic, etc.) from non-vinyl monomers; synthesis of chiral polymers; and a quantitative study, in both theoretical and experimental terms, of microtacticity and of its relationship with the mechanism of polymerization.

By an odd coincidence two contributions appeared in a single issue of this journal (September–October, 1982), both proving the existence of vinyl polymers with hitherto unobserved structures. These were the chiral copolymers having structure ...mrrmrrmrr... obtained by Wulff and Hohn[1] and the hemitactic polypropylene prepared by our own group.[2]

The aim of this paper is to illustrate the structural characteristics of hemitactic polymers and to outline the differences between these and conventional atactic polymers. A second article, published in this same issue,[3] illustrates an example of a hemitactic polymer—hemiisotactic polypropylene—and its usefulness in deepening our understanding of the ^{13}C NMR spectrum of polypropylene.

Hemitacticity and Hemiisotacticity

Following the definition given in the preceding article,[2] hemitactic polymers contain two distinct series of tertiary carbon atoms which alternate with each other: in the odd series the arrangement of the substituents is exactly defined, while in the even series their arrangement is random. In other words, only one tertiary carbon atom out of two is under the influence of an ordering rule. It was for this reason that we proposed the term *hemitactic* polymer to denote a sample of polypropylene having such a structure (hemi from the Greek: half).

A further step toward a structural characterization is to define the type of arrangement existing in the odd series. For example, the substituents bonded to carbons 1, 3, 5,

0024-9297/85/2218-0923$01.50/0